Multiphase modeling of nitrate photochemistry in the quasi-liquid layer (QLL): implications for NO$_x$ release from the Arctic and coastal Antarctic snowpack

C. S. Boxe and A. Saiz-Lopez

Earth and Space Science Division, NASA Jet Propulsion Laboratory, California Institute of Technology, Pasadena, CA 91109, USA

Correspondence to: C. S. Boxe (Christopher.Boxe@jpl.nasa.gov)

Abstract

We utilize a multiphase model, CON-AIR (Condense Phase to Air Transfer Model), to show that the photochemistry of nitrate (NO$_3^-$) in and on ice and snow surfaces, specifically the quasi-liquid layer (QLL), can account for NO$_x$ volume fluxes, concentrations, and [NO]/[NO$_2$](γ=[NO]/[NO$_2$]) measured just above the Arctic and coastal Antarctic snowpack. Maximum gas phase NO$_x$ volume fluxes, concentrations and γ simulated for spring and summer range from 5.0×10^4 to 6.4×10^5 molecules cm^{-3} s^{-1}, 5.7×10^8 to 4.8×10^9 molecules cm^{-3}, and ~0.8 to 2.2, respectively, which are comparable to gas phase NO$_x$ volume fluxes, concentrations and γ measured in the field. The model incorporates the appropriate actinic solar spectrum, thereby properly weighting the different rates of photolysis of NO$_3^-$ and NO$_2^-$. This is important since the immediate precursor for NO, for example, NO$_2^-$, absorbs at wavelengths longer than nitrate itself. Finally, one-dimensional model simulations indicate that both gas phase boundary layer NO and NO$_2$ exhibit a negative concentration gradient as a function of height although [NO]/[NO$_2$] are approximately constant. This gradient is primarily attributed to gas phase reactions of NO$_x$ with halogens oxides (i.e., as BrO and IO), HO$_x$, and hydrocarbons, such as CH$_3$O$_2$.

1 Introduction

Interest in the nitrogen cycle over the polar regions was revitalized due to elevated NO$_x$(NO+NO$_2$) levels detected in and above snowpacks (Honrath et al., 1999; Jones et al., 2000). Absorbing at $\lambda \geq 290$ nm, nitrate (NO$_3^-$) is one of the dominant anions present in the snowpack with approximately an even surface distribution with latitude and longitude at both polar regions (Legrand and Meyeski, 1997; Mulvaney et al., 1998). Due to production and long-range transport, nitrate concentrations at the Arctic (~10 μM) are higher than those measured at coastal Antarctica (~5 μM). Through solar photolysis, nitrate is a major source of NO$_x$ emissions from the snowpack. NO$_x$ mixing

ratios within and above the snowpack are proportional to NO_x production rates, time of day, and temperature (Cotter et al., 2003; Jones et al., 2000). Consequently, nitrate photochemistry has been the focus of a series of field (Honrath et al., 1999; Honrath et al., 2000a; Jones et al., 2000; Davis et al., 2001; Zhou et al., 2001; Dibb et al., 2002; Qiu et al., 2002; Honrath et al., 2002; Beine et al., 2002; Beine et al., 2003; Jacobi et al., 2004; Davis et al., 2004; Dibb et al., 2004) and laboratory experiments (Honrath et al., 2000b; Dubowski et al., 2001; Dubowski et al., 2002; Chu and Anastasio, 2003, Boxe et al., 2003; Boxe et al., 2005; Boxe et al., 2006; Jacobi et al., 2006; Jacobi and Hilker 2007).

If nitrate depth profiles in polar ice were preserved over time, they would provide a valuable record of global paleoatmospheres. However, physical and photochemical processing of nitrate can alter its surface and near-surface concentrations, especially at low-accumulation sites (Blunier et al., 2005), and possibly compromise its oxygen isotopic signature (McCabe et al., 2005). While the photochemistry of nitrate in the snowpack has significant implications for tropospheric chemistry, since its photoproducts, NO and NO_2, are intimately linked to reactions involving ozone, hydrocarbons and halogens, this process also generates OH radicals Reaction (R8), which can oxidize organic matter within snowpacks, leading to the formation of oxidized hydrocarbons (e.g., formaldehyde, acetaldehyde, acetone) (Dominé and Shepson, 1999; Sumner and Shepson, 2002; Grannas et al., 2004). In addition, HONO has been measured in the polar regions (Zhou et al., 2001; Honrath et al., 2002; Amoroso et al., 2006; Clemitshaw, 2006), where it has also been suggested as a possible byproduct of nitrate photolysis (Zhou et al., 2001). Yet, actual HONO concentrations and its source at polar sites have been debated (Chen et al., 2004; Dibb et al., 2004; Liao et al., 2006; Jacobi et al., 2007).

It is clear that overlying boundary layer chemistry is affected by photochemistry occurring at the snowpack at polar regions. A useful tool to study specified photochemical mechanisms occurring in the snowpack is to multiphase model boundary layer chemistry linked to chemistry at the snowpack surface, which requires a physicochemical

6011

understanding of ice surfaces. The ice-air interface of solids is an area that exhibits characteristics different from those of the bulk material. This is primarily due to the fact that atoms (or molecules) at the surface only encounter bonding forces with other molecules from one side; simultaneously, there is a similar imbalance at other interfaces. Furthermore, this behavior causes the dislocation of atoms from their original locations, alterations in their associated force and energy constants, and effects on layers below the ice-air demarcation.

The fact that the boundary between the solid and vapor phase is wetted by a thin liquid film causes the free energy of the boundary to be lower than it would be if the thin liquid film were absent (Dash et al., 1995). As a result, if the surface of ice were initially dry, then it would reduce its interfacial free energy by converting a layer (e.g., the surface) of the solid to liquid. Hence, a liquid-like layer should exist over some measurable and quantifiable temperature range on the surface of ice, below its bulk normal melting temperature. The existence of the QLL is not prohibited due to its thinness and closeness to the normal melting temperature of ice. The thickness of the QLL is present at a state where the free energy of the ice system is at a minimum and is governed by the competition between the free energy of the ice surface and the energy required to melt a solid layer.

The thickness of the QLL as a function of temperature has been quantified both experimentally (Doppenschmidt and Butt, 2000; Pittenger et al., 2001; Bluhm et al., 2002; Sadtchenko and Ewing, 2002) and theoretically (Ohnesorge et al., 1994; Landa et al., 1995; Wettlaufer, 1999). With the single exception of Elbaum et al. (1993), whose experiments were done on exposed horizontal facets in the prismatic orientation ($10\bar{1}0$), these studies have shown that the QLL increases with increasing temperature. Additionally, impurities enhance its thickness (Doppenschmidt and Butt, 2000; Wettlaufer, 1999). The addition of impurities at constant pressure will shift the normal melting point of the bulk solid, which is directly dependent on the concentration of the impurity. As the melting point is approached, the QLL appears to be indistinguishable from the liquid phase in its uppermost layers.

6012

The QLL can play a pivotal role in environmental phenomena such as 1) controlling the friction of ice and snow; 2) soil freezing, permafrost formation, and frost heave; 3) sintering and sliding in glaciers, sea-ice, and snow fields; and 4) behavior of atmospheric ice (Dash et al., 1995). The QLL has also been suggested to contribute to the electrification of thunder clouds via charge transfer at the liquid-ice interface (Baker and Dash, 1994). Abbatt et al. (1992) even proposed that polar stratospheric clouds are able to accommodate HCl by dissolution in multilayer-thick quasi-liquid films, where they can efficiently participate in ozone destruction during winter and spring months in Antarctica and the Arctic.

As shown in Jones et al. (2007), spring and summertime maximum NO_x volume fluxes range from $\sim 4.5 \times 10^4$ to $\sim 5.5 \times 10^5$ molecules cm^{-3} s^{-1}. In addition, field measurements of NO_x range from $\sim 5.7 \times 10^8$ to $\sim 2.9 \times 10^9$ molecules cm^{-3} and exhibit $[NO]/[NO_2]$ ($\gamma = [NO]/[NO_2]$) from ~ 0.8 to ~ 2.0 (Honrath et al., 1999; Jones et al., 2000; Beine et al., 2002; Dibb et al., 2002; Honrath et al., 2002; Simpson et al., 2007). In this study, we use CON-AIR to show that nitrate photochemistry in the QLL does simulate well NO_x volume fluxes, concentrations, and γ measured just above the snowpack (i.e., at ~ 25 cm) at various sites in the Arctic and coastal Antarctica. The implications of these findings are also discussed.

2 Model description

CON-AIR is a multiphase model that treats the interaction of gas phase boundary layer chemistry with condense phase chemistry and photochemistry in and on snow and ice surfaces, specifically the QLL. As described previously, here the QLL is defined as a thin layer on the surface of snow and ice, where water molecules are not in a rigid solid structure, yet not in the random order of a liquid (Petrenko and Whitworth, 1999), which, in our model, is the demarcation between the vapor and bulk ice phase. It is structured in two main components: i) condense phase chemistry and photochemistry regime in the QLL; and ii) gas phase chemistry scheme comprising photochemical,

6013

thermal, and heterogeneous reactions.

The exchange of nitrogen species between the QLL and the atmosphere depends on the respective Henry's law constants of species including NO and NO_2. The Henry's law solubility constants and temperature dependences for the gas phase equilibrating species NO and NO_2 are $1.9 \times 10^{-3} \times e^{(1500(1/T - 1/To))}$ M atm^{-1} and $6.4 \times 10^{-3} e^{(2500(1/T - 1/To))}$ M atm^{-1}, respectively (Schwartz and White, 1981; Lelieveld and Crutzen, 1991). The temperature dependence of the solubility of species is taken into account by including a diurnal variation of the typical temperature profile of both the Arctic and coastal Antarctic region during spring and summertime (i.e., $250 \leq T/K \leq 265$). A description of the radiation and gas phase scheme, and a complete set of all gas phase reactions employed in the model are summarized in Table 1 of the supplementary material. http://www.atmos-chem-phys-discuss.net/8/6009/2008/ acpd-8-6009-2008-supplement.pdf

2.1 Condense phase scheme and QLL parameterizations

As described in Saiz-Lopez and Boxe (2008), a description of the radiation and gas phase scheme, and a bulk concentrations of NO_3^- and NO_2^- at the Arctic and coastal Antarctic snowpack are $1 \leq [NO_3^-]/\mu M \leq 17$ and ~ 1 nM, respectively (Stotlemyer and Toczydlowski, 1990; Jaffe and Zukowski, 1993; Li, 1993; Silvente and Legrand, 1995; De Angelis and Legrand, 1995; Dibb et al., 1998; Jones et al., 2007). A number of laboratory experiments have provided evidence that the photolysis of nitrate transpires in the QLL on the surface of ice crystals (Dubowski et al., 2001; Dubowski et al., 2002; Boxe et al., 2003; Chu and Anastasio, 2003). In this study, we restrict our model simulations within the context that all condense phase reactions take place in the much smaller volume of the QLL. Typical bulk concentrations of NO_3^- and NO_2^- measured in the Arctic and coastal Antarctic snowpack were re-quantified following the formulation

6014

established by Cho et al. (2002). Cho et al. (2002) derived the following equation

$$\psi_{H_2O}(T) = \frac{m_{H_2O}RT_f}{1000H_f^0}\frac{T}{T_f - T}C_T^0, \tag{1}$$

which relates the fraction of liquid water (ψ_{H_2O}) as a function of temperature (T) and the total solute concentration in the QLL (C_T^0). $\psi_{H_2O}(T)$ is the fraction of water in the QLL as a function of temperature, m_{H_2O} is the molecular weight of water (18.01 g/mole), R is the gas constant (8.314×10^{-3} kJ/K mole), H_f^0 is enthalpy of fusion of water (6 kJ/mole), and T_f is the freezing temperature of water (273.15 K). Assuming that the total initial concentrations of NO_3^- and NO_2^- reside in the QLL, we relate their respective bulk concentrations (C_{bulk}) to their respective concentrations in the QLL via Eq. (2):

$$C_{bulk} = \psi_{H_2O}(T)C_T^0 \tag{2}$$

Substituting Eq. (1) into Eq. (2), yields the following:

$$\psi_{H_2O}(T) = \sqrt{\frac{m_{H_2O}RT_f}{1000H_f^0}\frac{T}{T_f - T}C_{bulk}} \, . \tag{3}$$

Then, given the upper limit $C_{bulk-upper-limit}$ (=17.0001 μM, $[NO_3^-]_o$=17 μM and $[NO_2^-]_o$=1 nM) and the lower limit $C_{bulk-lower-limit}$ (=1.0001 μM, $[NO_3^-]_o$=1 μM and $[NO_2^-]_o$=1 nM), we calculate 4.54×10^{-5} and 1.01×10^{-5} as the mean of the upper and lower limit ψ_{H_2O} from 250 to 265 K, respectively, by using Eqs. (4) and (5):

$$\text{mean of } \psi_{H_2O-upper-limit} = \frac{\sum_{i=250}^{i=265}\sqrt{\frac{m_{H_2O}RT_f}{1000H_f^0}\frac{T_i}{T_f-T_i}C_{bulk-upper-limit}}}{16}; \tag{4}$$

$$\text{mean of } \psi_{H_2O-lower-limit} = \frac{\sum_{i=250}^{i=265}\sqrt{\frac{m_{H_2O}RT_f}{1000H_f^0}\frac{T_i}{T_f-T_i}C_{bulk-lower-limit}}}{16} \, . \tag{5}$$

6015

Summing the mean of $\psi_{H_2O-upper-limit}$ and the mean of $\psi_{H_2O-lower-limit}$ gives 5.55×10^{-5}. In CON-AIR, as an approximation, we incorporate the average of this sum, 2.78×10^{-5}, as the fraction of liquid water, representative for temperatures from 250 to 265 K. Taking the mean of the median of $[NO_3^-]_o$ found in the Arctic (i.e., from 3 to 17 μM) and coastal Antarctic (i.e., from 1 to 9 μM) yields 7.5 μM. Then, as an estimation, we take $[NO_3^-]_o$=7.5 μM and $[NO_2^-]_o$=1 nM as their initial bulk concentrations. Using Eq. (2), the concentration of $[NO_3^-]_o$ and $[NO_2^-]_o$ in the QLL is 270 mM and 0.04 mM, respectively, which we incorporate in CON-AIR as their initial concentrations.

Given our estimated ψ_{H_2O}=2.78×10^{-5}, we calculate a QLL thickness $\sim$14 μm by the following formulation: mean snow depth $\times$ snow column cross-sectional area $\times$ mass fraction of liquid water = 54 cm $\times$ 1 cm^2 $\times$ 2.78×10^{-5}=0.05 cm^3; then, 0.00139 cm^3/1 cm^2=13.90 μm$\sim$14 μm.

Here, snow depth is defined as the total combined depth of both old and new below the snow-air interface. Using a mean snow depth of 54 cm and a snow density of 0.31 g cm^{-3} (Michalowski et al., 2000; Sumner and Shepson, 1999), the total potential liquid content in a snow column of 1 cm^2 cross-sectional area of snowpack is:

$$\text{total potential liquid content} = \frac{54 \text{ cm} \times 0.31 \text{ g cm}^{-3}}{1 \text{ g cm}^{-3}} = 16.74 \text{ cm}^3 \text{ cm}^{-2} \tag{6}$$

The estimated fraction of liquid water is 2.78×10^{-5}; therefore, the QLL volume on the snowpack surface is:

$$\text{QLL volume} = 16.74 \text{ cm}^3 \text{ cm}^{-2} \times 2.78 \times 10^{-5} = 4.65 \times 10^{-4} \text{ cm}^3 \text{ cm}^{-2} \tag{7}$$

To properly express aqueous phase reactions rates to QLL reaction rates, a volumetric factor (*volumetric*) was estimated based on laboratory derived reaction rate enhancement factors. A volumetric factor was quantified by taking the average of the upper limit reaction rate enhancement factors obtained in the laboratory by Grannas et al. (2007)

and Takenaka et al. (1996), 40 and 2.4×10^3, respectively, yielding

$$volumetric = \frac{40 + 2.4 \times 10^3}{2} = 1.22 \times 10^3 \tag{8}$$

Therefore, the reaction rates are quantified by incorporating volumetric factor, *volumetric*. The rate constants for reactions taking place in the QLL are:

$$k \times volumetric, \tag{9}$$

$$k \times volumetric^2, \tag{10}$$

where k are the actual literature aqueous phase rate constants in units of $cm^3 \, molecule^{-1} \, s^{-1}$ and $cm^6 \, molecule^{-2} \, s^{-1}$, for second- and third-order rate constants, respectively. Table 1 list the major reactions pertaining to nitrate photochemistry, their condense phase reaction rates, and their QLL reaction rates.

The rate constant for the transfer of species from the QLL to the gas phase is calculated using an approximation of the first order rate constant, $k_t = 1.25 \times 10^{-5} \, s^{-1}$ (Gong et al., 1997; Michalowski et al., 2000). For a boundary layer height of 100 m (10 000 cm)

$$k_{mix} = k_t \times \frac{4.65 \times 10^{-4} \, cm^3 \, (QLL)}{10\,000 \, cm^3 \, (atmosphere)} \tag{11}$$

Nevertheless, the rate of transfer of species will depend on the concentration and Henry's law constants for solubility of the corresponding species. Hence, the complete expression for the phase equilibration of species from the QLL to the atmosphere is:

$$k_{(QLL \to Atmosphere)} = (k_{mix} \times [\text{species concentration}])/(H') , \tag{12}$$

where H' is the dimensionless Henry's law constant. H' is defined as $H' = (HRT)$, where H is a species' Henry's law constant, R is the gas constant, $0.082058 \, L \, atm \, K^{-1} \, mol^{-1}$, and T is the temperature (K).

6017

3   Results and discussion

The photochemistry of nitrate in the aqueous phase has been studied extensively (Mark et al., 1996, Mack and Bolton, 1999). Dissolved nitrate has two primary absorption bands in the ultraviolet (UV). The first occurs in the far UV via the strong $\pi \to \pi*$ transition, centered at 201 nm ($\varepsilon_{max} = 9500 \, M^{-1} \, cm^{-1}$), and the second is a weaker absorption band that occurs via the highly forbidden $n \to \pi*$ transition, centered at 302 nm ($\varepsilon_{max} = 7.14 \, M^{-1} \, cm^{-1}$). Furthermore, it was proposed that the weaker absorption band may occur from the combination of a singlet and triplet $n \to \pi*$ and $\sigma \to \pi*$ transition (Maria et al., 1973).

Mack and Bolton (1999) showed that the overall stoichiometry for nitrate irradiation is

$$NO_3^- \xrightarrow{h\nu} NO_2^- + \frac{1}{2} O_2. \tag{R1}$$

In the absence of $\cdot OH$ scavengers this stoichiometry is maintained over the entire pH range (Wagner and Strehlow, 1980). For $\lambda < 280$ nm, the major reaction pathway is through isomerization of $[NO_3^-]*$, generated via Reaction (R2), to form $ONOO^-$, peroxynitrite, and at low pH, peroxynitrous acid, HONOO (R3). HONOO can also be produced from the recombination of $\cdot OH$ and NO_2 within a solvent cage as shown in Reaction (R4). HONOO isomerizes rapidly back to NO_3^- (R5) (Mack and Bolton, 1999).

$$NO_3^- \xrightarrow{h\nu} [NO_3^-]* \tag{R2}$$

$$NO_3^- \longrightarrow ONOO^- + H^+ + \longrightarrow HONOO \tag{R3}$$

$$\cdot OH + NO_2 \longrightarrow HONOO \tag{R4}$$

$$HONOO \longrightarrow NO_3^- + H^+ \tag{R5}$$

Yet, in the troposphere, all $\lambda < 290$ nm is completely attenuated by stratospheric ozone. Therefore, $\lambda \geq 290$ nm are pertinent for this study. In aqueous solutions at pH<6 and

6018

$\lambda \geq 290$ nm, nitrate photolysis proceeds via two primary photolytic pathways as illustrated in Reactions (R6) and (R7), through the generation of nitrate in the excited state, $[NO_3^-]*$, from Reaction (R2). As shown in Reaction (R8), O^- reacts rapidly with water to form the hydroxyl radical.

$$[NO_3^-]* + H^+ \longrightarrow NO_2 + O^- \tag{R6}$$

$$[NO_3^-]* \longrightarrow NO_2^- + O(^3P) \tag{R7}$$

$$O^- + H_2O \longrightarrow \cdot OH + OH^- \tag{R8}$$

Atomic oxygen produced in Reaction (R7) can react with molecular oxygen ($[O_2]_{water} \sim 0.3$ mM) via Reaction (R9) or with nitrate by way of Reaction (R10) (Warneck and Wurzinger, 1988).

$$O_2 + O(^3P) \longrightarrow O_3 \tag{R9}$$

$$NO_3^- + O(^3P) \longrightarrow NO_2^- + O_2 \tag{R10}$$

Ozone, generated by Reaction (R9), is either consumed by reaction with NO_2^- (R11) (Hoigne et al., 1985) or by decomposition to $\cdot OH$ (Hoigne et al., 1985).

$$NO_2^- + O_3 \longrightarrow NO_3^- + O_2 \tag{R11}$$

The UV absorption spectrum of nitrite displays three absorption bands: the first involves a $\pi \rightarrow \pi*$ transition with maxima at 220 nm, and the latter two peaks are maxima at 318 nm (ε_{max}=10.90 M^{-1} cm^{-1}) and 354 nm (ε_{max}=22.90 M^{-1} cm^{-1}), both corresponding to $n \rightarrow \pi*$ transitions. Similar to nitrate, nitrite undergoes direct photolysis as shown in Reaction (R12) to produce NO, and it also oxidizes by reaction with $\cdot OH$ via Reaction (R13).

$$NO_2^- + H^+ \xrightarrow{h\nu} NO + \cdot OH \tag{R12}$$

$$NO_2^- + \cdot OH \longrightarrow NO_2 + OH^- \tag{R13}$$
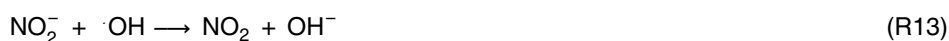
The photolysis of NO_2 also produces NO (R14). We exclude this reaction from the chemical scheme used in CON-AIR since its photolytic lifetime during midday spring and summertime ($1/J_{NO_2}$=1/4.6×10^{-3} $sec^{-1} \approx$ 217 sec) (Yung and DeMore, 1999) is longer than its diffusion lifetime through a 14 μm (or 14×10^{-4} cm) thick QLL. As calculated using the diffusion length Eq. (13) (Dubowski et al., 2001):

$$NO_2 \xrightarrow{h\nu} NO + O(^3P) \tag{R14}$$

$$L = \sqrt{D\tau} \quad ; \tau = \frac{(14 \times 10^{-4} cm)^2}{9.8 \times 10^{-9}\ cm^2 s^{-1}} \approx 200\ sec \tag{13}$$

L is the thickness of the QLL, D is the diffusion coefficient of NO_2 [Dubowski et al., 2001], and τ is the time it takes NO_2 to diffuse through a thickness L. Using Eq. (13) shows that the maximum ice layer thickness where NO_2 photolysis will not occur is $\approx (9.8 \times 10^{-9}\ cm^2\ s^{-1} \times 217\ s)^{1/2} \approx 15\ \mu$m. This estimation is further supported by previous findings, which have shown that NO_2 produced from nitrate photolysis in the outermost layers of thin ice films are readily released to the gas phase, compared to NO_2 formed at deeper depths, which undergoes further chemical and photolytic processing [Dubowski et al., 2001; Boxe et al., 2005; Boxe et al., 2006]. Finally, the photoproduced NO and NO_2 are readily released to the gas phase after equilibration due to their low solubility (R15).

$$NO_{2(QLL)}, NO_{(QLL)} \xrightarrow{escape} NO_{2(g)}, NO_{(g)} \tag{R15}$$

The protonation of nitrite to form nitrous acid ($HONO_{(aq)}$) (R16) was also not considered in the QLL reaction mechanism since model simulations yielded $\gamma \sim 1500$, much larger than any reported measurements from field studies (e.g., $\gamma \sim 0.8$ to ~ 2.0) [Honrath et al., 1999; Jones et al., 2000; Beine et al., 2002; Dibb et al., 2002; Honrath et al., 2002; Jones et al., 2007; Simpson et al., 2007]. This result implies that a significant amount of

HONO produced in the snowpack may be retained by matrix or solvent cage effects or may be dependent on photosensitized organic compounds, such as possible reaction cycles that may efficiently transfer electrons to NO_2, possibly leading the production of HONO (Beine et al., 2006). Presently, the mechanism of HONO formation from NO_3^-, is not well known.

$$NO_2^- + H^+ \longrightarrow HONO_{(aq)} \Leftrightarrow HONO_{(g)} \tag{R16}$$

A simplified scheme illustrating the primary reactions governing NO_x release from the QLL film to the gas phase from nitrate photochemistry used in CON-AIR is shown in Fig. 1. Laboratory studies have shown that the photochemistry of nitrate in ice is analogous to its aqueous phase photochemistry (Dubowski et al., 2001; Dubowski et al., 2002; Chu and Anastasio et al., 2003; Boxe et al., 2006) Therefore, as shown in Table 1, QLL reaction rates were quantified by scaling aqueous phase reaction rates according to the micro-scopic dimensions of the QLL.

Laboratory studies have shown that nitrate is a source of NO and NO_2 from ice surfaces (Honrath et al., 2000b; Dubowski et al., 2001; Dubowski et al., 2002; Chu and Anastasio, 2003; Boxe et al., 2003; Boxe et al., 2005; Boxe et al., 2006; Jacobi et al., 2006; Jacobi and Hilker 2007). Only a small number of laboratory investigations of nitrate photochemistry in ice were carried out to correlate their respective NO and NO_2 fluxes with field measurements (Boxe et al., 2003; Boxe et al., 2006). Yet, these studies were restricted by high detection limits for NO and NO_2 and the use of irradiation sources emitting at 313±20 nm (i.e., overlapping the absorption spectrum of nitrate), resulting in higher NO_x concentrations than measured in the field and much lower γ (e.g., 0.043 to 0.0005) than those measured over the Arctic and Antarctic snowpack (Boxe et al., 2003; Boxe et al., 2006). Compared to the typical initial nitrate concentrations (1 to 17 μM) and the typical actinic flux spectrum at Earth's surface for the Arctic and coastal Antarctic regions, the higher initial nitrate concentrations (50 mM) and the dissimilar actinic flux spectrum used, likely contributed to the disparity between these laboratory results and those from the field. Figure 2 illustrates this disparity to some extent by comparing the absorption spectrum for nitrate and nitrite and the actinic flux

6021

spectrum at the Earth's surface. The surface irradiance is computed using a 2-stream radiative transfer code (Thompson, 1984). We calculate the diurnal variation of $J_{NO_3^-}$ and $J_{NO_2^-}$ for snowpack summer and springtime conditions by extrapolating laboratory modeled and measured $J_{NO_3^-}$ and $J_{NO_2^-}$ for ice, snowpack, and seawater (Zuo and Deng, 1998; Qiu et al., 2002; King et al., 2005) to the radiative transfer code, coupled to CON-AIR, such that $J_{NO_3^-}$ and $J_{NO_2^-}$ vary as a function of solar zenith angle (or as a function of time of day), therefore providing a more complete representation of nitrate photochemistry. Note, the smaller and larger summer/springtime diurnal profiles of $J_{NO_3^-}$ were derived from extrapolating the lower and upper limits for the $J_{NO_3^-}$ values obtained for surface snow and sea-ice (Qiu et al., 2002; King et al., 2005), while the summer/springtime diurnal profile of $J_{NO_2^-}$ was derived from extrapolating the $J_{NO_2^-}$ value obtained for surface seawater (Zuo and Deng, 1998). Figure 3 illustrates a typical diurnal profile for NO (e.g., maximum volume fluxes of 2.3×10^4 molecules cm^{-3} s^{-1} during spring and 3.2×10^5 molecules cm^{-3} s^{-1} during summer) and NO_2 (e.g., maximum concentrations of 1.2×10^4 molecules cm^{-3} s^{-1} to 2.7×10^4 molecules cm^{-3} s^{-1} during spring and 1.8×10^5 to 3.2×10^5 molecules cm^{-3} s^{-1} during summer) over the Arctic and Antarctic snowpack. These simulated NO_x volume fluxes are comparable to field measurements of Jones et al. (2007). Assuming a ~100 m boundary height and taking the median of the concentration of molecules between 250 and 265 K at atmospheric surface pressure (1 atm or 1.01325×10^5 N m^{-2}) (2.86×10^{19} molecules cm^{-3}), simulated maximum concentrations of NO_x, ~5.7×10^8 to ~4.8×10^9 molecules cm^{-3}, agree well with maximum concentrations of NO_x measured just above the snowpack by field measurements, ~5.7×10^8 to ~2.9×10^9 molecules cm^{-3}, (Honrath et al., 1999; Jones et al., 2000; Beine et al., 2002; Dibb et al., 2002; Honrath et al., 2002; Simpson et al., 2007). It also accounts for the range of γ measured during Arctic and Antarctic summer and springtime, where springtime maximum γ ranges from ~0.84 to ~1.86 and summertime maximum γ ranges from ~0.50 to ~2.20, which is also in good accord with measured γ over the snowpack (Honrath et al., 1999; Jones et al., 2000; Beine et al., 2002; Dibb et

6022

al., 2002; Honrath et al., 2002; Simpson et al., 2007). Furthermore, these findings reinforce the fact that the immediate precursor for NO, likely NO_2^-, absorb at wavelengths longer than nitrate itself, as shown in Fig. 2; thus, incorporating the actinic flux at the Earth's surface shows that nitrite is more photolabile than nitrate (Cotter et al., 2003).

Furthermore, we investigate the profile of gas phase boundary layer NO and NO_2 as a function of height up to 20 m during the summertime over the snowpack using a 1-D model (Saiz-Lopez et al., 2007). Figure 4 shows that the model predicts a slight negative gradient for both [NO] and [NO_2], and γ remains approximately constant. The gradient is the result of gas phase reactions of NO_x with halogens oxides (i.e., BrO and IO), HO_x, and hydrocarbons (e.g., CH_3O_2) (Saiz-Lopez et al., 2007). Atmospheric stability and wind speed may also affect the concentration gradient of NO_x above the snowpack (Beine et al., 2002). However, constraining the 1-D model with the lower limit summertime NO and NO_2 volume fluxes derived from CON-AIR leads to good agreement with recent summertime observations of NO and NO_2 concentrations (13 ppt and 7 ppt as average noon values) and ratios ([NO]/[NO_2] ~1.8) obtained at a few meters above the coastal Antarctic snowpack (e.g., Jones et al., 2007).

References

Amoroso, A., Beine, H. J., Sparapani, R., Nardino, M., and Allegrini, I.: Observations of co-inciding arctic boundary layer ozone depletion and snow surface emissions of nitrous acid, Atmos. Environ., 40, 1949–1956, 2006.

Baker, M. B. and Dash, J. G.: Mechanism of change-transfer between colliding ice particles in thunderstorms, J. Geophys. Res.-Atmos., 99, 10 621–10 626, 1994.

6023

Beine, H. J., Honrath, R. E., Dominé, F., Simpson, W. R., and Fuentes, J. D.: NO_x during background and ozone depletion periods at Alert: fluxes above the snow surfaces, J. Geophys. Res., 107, 4584, doi:10.1029/2002JD002082, 2002.

Beine, H. J., Dominé, F., Ianniello, A., Nardion, M., Allegrini, I., Teinila, K., and Hillamo, R.: Fluxes of nitrate between snow surfaces and the atmosphere in the European high Arctic, Atmos. Chem. Phys., 3, 335–346, 2003,
http://www.atmos-chem-phys.net/3/335/2003/.

Beine, H. J., Amoroso, A., Dominé, F., King, M. D., Nardino, M., Ianniello, A., and France, J. L.: Surprisingly small HONO emissions from snow surfaces at Browning Pass, Antarctica, Atmos. Chem. Phys., 6, 2569–2580, 2006,
http://www.atmos-chem-phys.net/6/2569/2006/.

Bluhm, H., Olgetree, D. F., Fadley, C. S., Hussain, Z., and Salmeron, N.: The premelting of ice studied with photoelectron spectroscopy, J. Phys.-Condens. Mat., 14, L227–L233, 2002.

Blunier, T., Floch, G. L., Jacobi, H.-W., and Quansah, E.: Isotopic view on nitrate loss in Antarctic surface snow, Geophys. Res. Lett., 32, L13501, doi:10.1029/2005GL023011, 2005.

Boxe, C. S., Colussi, A. J., Hoffmann, M. R., Tan, D., Mastromarino, J., Case, A. T., Sandholm, S. T., and Davis, D. D.: Multiscale ice fluidity in NO_x photodesorption from frozen nitrate solutions, J. Phys. Chem. A, 107, 11 409–11 413, 2003.

Boxe, C. S., Colussi, A. J., Hoffmann, M. R., Murphy, J. G., Wooldridge, P. J., Betram, T. H., and Cohen, R. C.: Photochemical production and release of gaseous NO_2 from nitrate-doped water ice, J. Phys. Chem. A, 109, 8520–8525, 2005.

Boxe, C. S., Colussi, A. J., Hoffmann, M. R., Perez, I. M., Murphy, J. G., and Cohen, R. C.: Kinetics of NO and NO_2 evolution from illuminated frozen nitrate solutions, J. Phys. Chem. A, 110, 3578–3583, 2006.

Chen, G., Davis, D., Crawford, J., Hutterli, L. M., Huey, L. G., Slusher D., Mauldin, L., Eisele, F., Tanner, D., Dibb, J., Buhr, M., McConnell, J., Lefer, B., Shetter, R., Blake, D., Song, C. H., Lombardi, K., and Arnoldy, J.: A reassessment of HO_x South Pole chemistry based on observations recording during ISCAT 2000, Atmos. Environ., 38, 5451–5461, 2004.

Cho, H., Shepson, P. B., Barrie, L. A., Cowin, J. P., and Zaveri, R.: NMR investigations of the quasi-brine layer in ice/brine mixtures, J. Phys. Chem. B, 106, 11 226–11 232, 2002.

Chu, L. and Anastasio, C.: Quantum yields of hydroxyl radical and nitrogen dioxide from the photolysis of nitrate on ice, J. Phys. Chem. A, 107, 9594–9602 2003.

Clemitshaw, K. C.: Coupling between the tropospheric photochemistry of nitrous acid (HONO)

6024

and nitric acid (HNO$_3$), Environ. Chem., 3, 31–34, 2006.

Cotter, E. S. N., Jones, A. E., Wolff, E. W., and Baugitte, S. J.-B.: What controls photochemical NO and NO$_2$ production from Antarctic snow? Laboratory investigation assessing the wavelength and temperature dependence, J. Geophys. Res., 108, 4147, doi:10.1029/2002JD002602, 2003.

Dash, J. G., Fu, H. Y., and Wettlaufer, J. S.: The premelting of ice and its environmental consequences, Rep. Prog. Phys., 58, 115–167, 1995.

Davis, D., Nowak, J. B., Chen, G., Buhr, M., Arimoto, R., Hogan, A., Eisele, F., Mauldin, L., Tanner, D., Shetter, R., Lefer, B., and McMurry, P.: Unexpected high levels of NO observed at South Pole, Geophys. Res. Lett., 28, 3625–3628, 2001.

Davis, D., Chen, G., Buhr, M., Crawford, J., Lenschow, D., Lefer, B., Shetter, R., Eisele, F., Mauldin, L., and Hogan, A.: South Pole NO$_x$ chemistry: an assessment of factors controlling variability and absolute levels, Atmos. Environ., 38, 5375–5388, 2004.

De Angelis, D. and Legrand, M.: Preliminary investigations of post-depositional effects of HCl, HNO$_3$, and organic acids in polar firn layers, in Ice Core Studies of Global Biogeochemical Cycles, edited by Delmas, R. J., NATO ASI Ser., Ser. I, vol. 30, Springer-Verlag, New York, 361–381, 1995.

Dibb, J. E., Arsenault, M., Peterson, M. C., and Honrath, R. E.: Fast nitrogen oxide photochemistry in Summit, Greenland snow, Atmos. Environ., 36, 2501–2511, 2002.

Dibb, J. E., Huey, G. L., Slusher, D. L., and Tanner, D. J.: Soluble reactive nitrogen oxides at South Pole during ISCAT 2000, Atmos. Environ., 38, 5399–5409, 2004.

Dominé, F. and Shepson, P. B.: Air-snow interactions and atmospheric chemistry, Science, 297, 1506–1510, 2002.

Doppenschmidt, A. and Butt, H. J.: Measuring the thickness of the liquid-like layer on ice surfaces with atomic force microscopy, Langmuir, 16, 6709–6714, 2000.

Dubowski, Y., Colussi, A. J., and Hoffmann, M. R.: Nitrogen dioxide release in the 302 nm band photolysis of spray-frozen aqueous nitrate solutions, Atmospheric implications, J. Phys. Chem. A., 105, 4928–4932, 2001.

Dubowski, Y., Colussi, A. J., Boxe, C., and Hoffmann, M. R.: Monotonic increase of nitrite yields in the photolysis of nitrate in ice and water between 238 and 294 K, J. Phys. Chem., 106, 6967–6971, 2002.

Gaffney, J. S., Marley, N. A., and Cunningham, M. M.: Measurement of the absorption constants for nitrate in water between 270 and 335 nm, Environ. Sci. Technol., 25, 207–209, 1992.

Gong, S. L., Walmsley, J. L., Barrie, L. A., and Hopper, J. F.: Mechanisms for surface ozone depletion and recovery during Polar Sunrise, Atmos. Environ., 31(7), 969–981, 1997.

Grannas, A. M., Shepson, P. B., and Filley, T. R.: Photochemistry and nature of organic matter in Arctic and Antarctic snow, Global Biogeochem. Cy., 18, doi:10.1029/2003GB002133, 2004.

Grannas, A. M., Bausch, A. R., and Mahanna, K. M.: Enhanced aqueous photochemical reaction rates after freezing, J. Phys. Chem. A, 111, 11 043–11 049, 2007.

Hoigne, J., Bader, H., Haag, W. R., and Staehelin, J.: Rate constants of reactions with organic and inorganic compounds in water-III, Inorganic compounds and radicals, Water Res., 19, 993–1004, 1985.

Honrath, R. E., Peterson, M. C., Guo, S., Dibb, J. E., Shepson, P. B., and Campbell, B.: Evidence of NO$_x$ production within or upon ice particles in the Greenland snowpack, Geophys. Res. Lett., 26, 695–698 1999.

Honrath, R. E., Peterson, M. C., Dziobak, M. P., Dibb, J. E., Arsenault, M. A., and Green, S. A.: Release of NO$_x$ from sunlight-irradiated midlatitude snow, Geophys. Res. Lett., 26, 695–698, 2000a.

Honrath, R. E., Guo, S., Peterson, M. C., Dziobak, M. P., Dibb, J. E., and Arsenault, M. A.: Photochemical production of gas phase NO$_x$ from ice crystal NO$_3^-$, J. Geophys. Res., 105, 24 183–24 190, 2000b.

Honrath, R. E., Lu, Y., Peterson, M. C., Dibb, J. E., Arsenault, M. A., Cullen, N. J., and. Steffen, K.: Vertical fluxes of NO$_x$, HONO, and HNO$_3$ above the snowpack at Summit, Greenland, Atmos. Environ., 36, 2629–2640, 2002.

Jacobi, H.-W., Bales, R. C., Honrath, R. E., Peterson, M. C., Dibb, J. E., Swanson, A. L., and Albert, M. R.: Reactive trace gases measured in the interstitial air of surface snow at Summit, Greenland, Atmos. Environ., 38, 1687–1697, 2004.

Jacobi, H.-W., Annor, T., and Quansah, E.: Investigation of the photochemical decomposition of nitrate, hydrogen peroxide, and formaldehyde in artificial snow, J. Photochem. Photobiol. A., 179, 330–338, 2006.

Jacobi, H.-W. and Hilker, B.: A mechanism for the photochemical transformation of nitrate in snow, J. Photochem. Photobiol. A, 185, 371–382, 2007.

Jaffe, D. A. and Zukowski, M. D.: Nitrate deposition to the Alaska snowpack, Atmos. Environ., 27A, 2935–2941, 1993.

Jones, A. E., Weller, R., Wolff, E. W., and Jacobi, H.-W.: Speciation and rate of photochemical NO and NO$_2$ production from Antarctic snow, Geophys. Res. Lett., 27, 345–348, 2000.

Jones, A. E., Wolff, E. W., Ames, D., Bauguitte, S. J.-B., Clemitshaw, K. C., Fleming, Z., Mills, G. P., Saiz-Lopez, A., Salmon, R. A., Sturges, W. T., and Worton, D. R.: The multi-seasonal NOy budget in coastal Antarctica and its link with surface snow and ice core nitrate: results from the CHABLIS campaign, Atmos. Chem. Phys. Discuss., 7, 4127–4163, 2007, http://www.atmos-chem-phys-discuss.net/7/4127/2007/.

King, M. D., France, J. L., Fisher, F. N., and Beine, H. J.:Measurement and modeling of UV radiation penetration and photolysis rates of nitrate and hydrogen peroxide in Antarctic sea ice: An estimate of the production rate of hydroxyl radicals in first-year sea ice, J. Photochem. Photobiol. A, 176, 39–49, 2005.

Legrand, M. and Mayewski, P.: Glaciochemistry of polar ice cores: a review, Rev. Geophys., 35, 219–243, 1997.

Landa, A., Wynblatt, P., Hakkinen, H., Barnett, R. N., and Landman, U.: Equilibrium interphase interfaces and premelting of the Pb(110) surface, Phys. Rev. B, 51, 10 972–10 980, 1995.

Lelieveld, J. and Crutzen, P. J.: The role of clouds in tropospheric photochemistry, J. Atmos. Chem., 12, 229–267, 1991.

Li, S.-M.: Particulate and snow nitrite in the spring arctic troposphere, Atmos. Environ., 27, 2959–2967, 1993.

Liao, W., Case, A. T., Mastromarino, J., Tan, D., and Dibb, J. E.: Observations of HONO by laser-induced fluorescence at the Sout Pole during ANTCI 2003, Geophys. Res. Lett., 33, L09810, doi:10.1029/2005GL025470, 2006.

Mack, J. and Bolton, J. R.: Photochemistry of nitrite and nitrate in aqueous solution: a review, J. Photochem. Photobiol. A, 128, 1–13, 1999.

Maria, H. J., McDonald, J. R., and McGlynn, S. P.: Electronic absorption spectrum of nitrate ion and boron trihalides, J. Am. Chem. Soc., 95, 1050–1056, 1973.

Mark, G., Korth, H.-G., Schuchmann, H.-P., and von Sonntag, C.: The photochemistry of aqueous nitrate ion revisited, J. Photochem. Photobiol. A, 101, 89–103, 1996.

McCabe, J. R., Boxe, C. S., Colussi, A. J., Hoffmann, M. R., and Thiemens, M. H.: Oxygen isotopic fractionation in the photochemistry of nitrate in water and ice, J. Geophys. Res., 110, D15310, doi:10.1029/2004JD005484, 2005.

Michalowski, B. A., Francisco, J. S., Li, S.-M., Barrie, L. A., Bottenheim, J. W., Shepson P. B.:A computer model study of multiphase chemistry in the Arctic boundary layer during polar sunrise, J. Geophys. Res., 105, 15 131–15 145, 2000.

Mulvaney, R., Wagenback, D., and Wolff, E. W.: Postdepositional change in snowpack nitrate

6027

from observation of year-round near-surface snow in coastal Antarctica, J. Geophys. Res., 103, 11 021–11 031, 1998.

Ohnesorge, R., Lowen, H., and Wagner, H.: Density-Functional theory of crystal fluid interfaces and surface melting, Phys. Rev. E, 50, 4801–4809, 1994.

Petrenko, V. F. and Whitworth, R. W.: Physics of Ice, Oxford University Press, New York, 1999.

Pittenger, B., Fain, S. C., Cochran, M. J., Donev, J. M. K., Robertson, B. E., Szuchmacher, A., and Overney, R. M.: Premelting at ice-solid interfaces studied via velocity-dependent indentation with force microscope tips, Phys. Rev. B, 63, Art. No. 134102, 134102-1–134102-15, 2001.

Qiu, R., Green, S. A., Honrath, R. E., Peterson, M. C., Lu, Y., and Dziobak, M.: Measurements of $J_{NO_3^-}$ in snow by nitrate-based actinometry, Atmos. Environ., 36, 2563–2571, 2002.

Sadtchenko, V. and Ewing, G. E.: Interfacial melting of thin ice films: An infrared study, J. Chem. Phys., 116, 4686–4697, 2002.

Saiz-Lopez, A., Plane, J. M. C., Mahajan, A. S., Anderson, P. S., Bauguitte, S. J.-B., Jones, A. E., Roscoe, H. K., Salmon, R. A., Bloss, W. J., Lee, J. D., and Heard, D. E.: On the vertical distribution of boundary layer halogens over coastal Antarctica: implications for O_3, HO_x, NO_x, and the Hg lifetime, Atmos. Chem. Phys. Discuss., 7, 9385–9417, 2007, http://www.atmos-chem-phys-discuss.net/7/9385/2007/.

Saiz-Lopez, A., and Boxe, C. S.: A mechanism for biologically-induced iodine emissions from sea-ice, Atmos. Chem. Phys. Discuss., 8, 2953–2976, 2008, http://www.atmos-chem-phys-discuss.net/8/2953/2008/.

Schwartz, S. E. and White, W. H.: Solubility equilibria of the nitrogen oxides and oxyacids in dilute aqueous solution, in: Advances in Environmental Science and Engineering, edited by: Pfafflin, J. R. and Ziegler, E. N., 4, 1–45, 1981.

Silvente, E. and Legrand, M.: A preliminary study of air-snow relationship for nitric acid in Greenland, in Ice Core Studies of Global Biogeochemical Cycles, NATO ASI Ser., Ser. I, vol. 30, edited by Delmas, R. J. , Springer-Verlag, New York, 225–240, 1995.

Simpson, W. R., von Glasow, R., Riedel, K., Anderson, P., Bottenheim, J., Burrows, J., Carpenter, L. J., Frieß, Goodsite, M. E., Heard, D., Hutterli, M., Jacobi, H.-W., Kaleschke, L., Neff, B., Plane, J., Platt, U., Richter, A., Roscoe, H., Sander, R., Shepson, P., Sodeau, J., Steffen, A., Wagner T., and Wolff, E.: Halogens and their role in polar boundary-layer ozone depletion, Atmos. Chem. Phys., 7, 4375–4418, 2007, http://www.atmos-chem-phys.net/7/4375/2007/.

6028

Stottlemeyer, R. and Toczydlowski, D.: Pattern of solute movement from snow into an Upper Michigan stream, Can. J. Fish. Aquat. Sci., 47, 290–300, 1990.

Sumner, A. L. and Shepson, P. B.: Snowpack production of formaldehyde and its effect on the Arctic troposphere, Nature, 398, 230–233, 1999.

[5] Takenaka, N., Ueda, A., Daimon, T., Bandow, H., Dohmaru, T., and Maeda, Y.: Acceleration mechanism of chemical reaction by freezing: the reaction of nitrous acid with dissolved oxygen, J. Phys. Chem., 100, 13 874–13 884, 1996.

Thompson, A. M.: The effects of clouds on photolysis rates and ozone formation in the unpolluted troposphere, J. Geophys. Res.-Atmos, 89, 1341–1349, 1984.

[10] Wagner, I. and Strehlow, H. Z.: Flash photolysis of nitrate ions in aqueous solutions, Phys. Chemie, Neue Folge, 123, 1–33, 1980.

Warneck, P. and Wurzinger, C.: Product quantum yields for the 305-nm photodecomposition of NO_3^- in aqueous solution, J. Phys. Chem., 92, 6278–6283, 1988.

Wettlaufer, J. S.: Impurity effects in the premelting of ice, Phys. Rev. Lett., 82, 2516–2519, [15] 1999.

Yung, Y. L. and Demore, W. B.: Photochemistry of Planetary Atmospheres, Oxford University Press, 1999.

Zhou, X., Beine, H. J., Honrath, R. E., Fuentes, J. D., Simpson, W., Shepson, P. B., and Bottenheim, J. W.: Snowpack photochemical production of HONO: a major source of OH in [20] the arctic boundary layer in springtime, Geophys. Res. Lett., 28, 4087–4090, 2001.

Zuo, Y. and Y. Deng, Y.: The near-UV absorption constants for nitrite ion in aqueous solution, Chemosphere, 36, 181–188, 1998.

6029

Table 1. QLL Reactions and Rate Constants

Reactions	Aqueous Rate Constants[a]	QLL Rate Constants[b]
$NO_3^- + h\nu \rightarrow NO_2 + O^-$		[c]
$NO_3^- + h\nu \rightarrow NO_2^- + O(^3P)$		[c]
$NO_2^- + h\nu \rightarrow NO + O^-$		[d]
$O^- + H_2O \rightarrow \cdot OH + OH^-$	2.82×10^{-15} cm^3 molec^{-1} s^{-1}	2.82×10^{-15} cm^3 molec^{-1} s^{-1}/(volumetric)[e]
$\cdot OH + OH^- \rightarrow O^- + H_2O$	2.00×10^{-11} cm^3 molec^{-1} s^{-1}	2.00×10^{-11} cm^3 molec^{-1} s^{-1}/(volumetric)[e]
$O_2 + O(^3P) \rightarrow O_3$	6.64×10^{-12} cm^3 molec^{-1} s^{-1}	6.64×10^{-12} cm^3 molec^{-1} s^{-1}/(volumetric)[e]
$O(^3P) + NO_2^- \rightarrow NO_3^-$	2.46×10^{-12} cm^3 molec^{-1} s^{-1}	2.46×10^{-12} cm^3 molec^{-1} s^{-1}/(volumetric)[e]
$O_3 + NO_2^- \rightarrow NO_3^- + O_2$	6.15 x 10^{-16} cm^3 molec^{-1} s^{-1}	6.15 x 10^{-16} cm^3 molec^{-1} s^{-1}/(volumetric)[e]
$NO_3^- + O(^3P) \rightarrow NO_2^- + O_2$	3.72×10^{-13} cm^3 molec^{-1} s^{-1}	3.72×10^{-13} cm^3 molec^{-1} s^{-1}/(volumetric)[e]
$NO_2^- + \cdot OH \rightarrow NO_2 + OH^-$	3.32×10^{-11} cm^3 molec^{-1} s^{-1}	3.32×10^{-11} cm^3 molec^{-1} s^{-1}/(volumetric)[e]
$NO_2 + NO_2 + H_2O \rightarrow NO_2^- + NO_3^- + 2H^+$	1.66×10^{-13} cm^3 molec^{-1} s^{-1}	1.66×10^{-13} cm^3 molec^{-1} s^{-1}/(volumetric)[e]
$NO + NO_2 + H_2O \rightarrow 2NO_2^- + 2H^+$	3.32×10^{-13} cm^3 molec^{-1} s^{-1}	3.32×10^{-13} cm^3 molec^{-1} s^{-1}/(volumetric)[e]
$NO + \cdot OH \rightarrow NO_2^- + H^+$	3.32×10^{-11} cm^3 molec^{-1} s^{-1}	3.32×10^{-11} cm^3 molec^{-1} s^{-1}/(volumetric)[e]
$NO_2 + \cdot OH \rightarrow NO_3^- + H^+$	2.16×10^{-12} cm^3 molec^{-1} s^{-1}	2.16×10^{-12} cm^3 molec^{-1} s^{-1} (volumetric)[e]
$NO + NO_2 \rightarrow N_2O_3$	1.83×10^{-12} cm^3 molec^{-1} s^{-1}	1.83×10^{-12} cm^3 molec^{-1} s^{-1}/(volumetric)[e]
$N_2O_3 + H_2O \rightarrow 2NO_2^- + 2H^+$	5.3×10^2 s^{-1}	5.3×10^2 s^{-1}
$2NO_2 \rightarrow N_2O_4$	7.48×10^{-13} cm^3 molec^{-1} s^{-1}	7.48×10^{-13} cm^3 molec^{-1} s^{-1}/(volumetric)[e]
$N_2O_4 + H_2O \rightarrow NO_2^- + NO_3^- + 2H^+$	10^3 s^{-1}	10^3 s^{-1}

[a] Aqueous phase reaction rate constants were obtained from Mack and Bolton (1999).

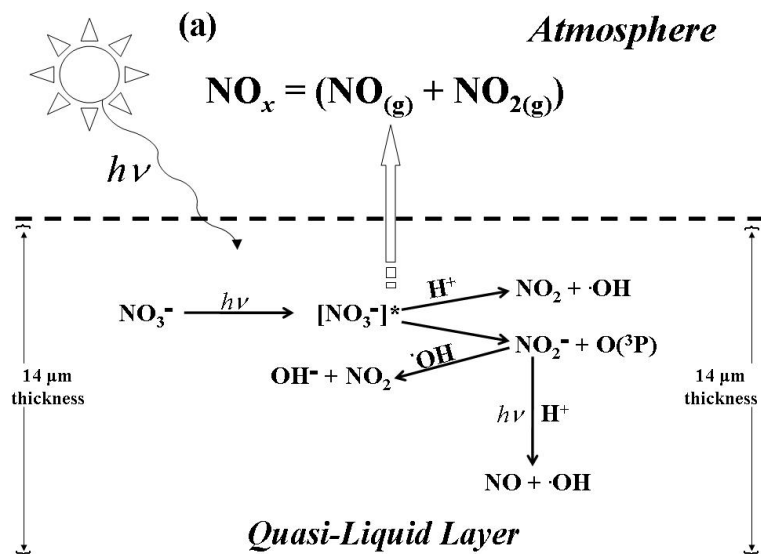[b] QLL rate reaction rate constants were quantified by including the "volumetric" factor (Michalowski et al., 2000).

[c] $J_{NO_3^-}$ values were extrapolated from Qui et al. (2002) and King et al. (2005).
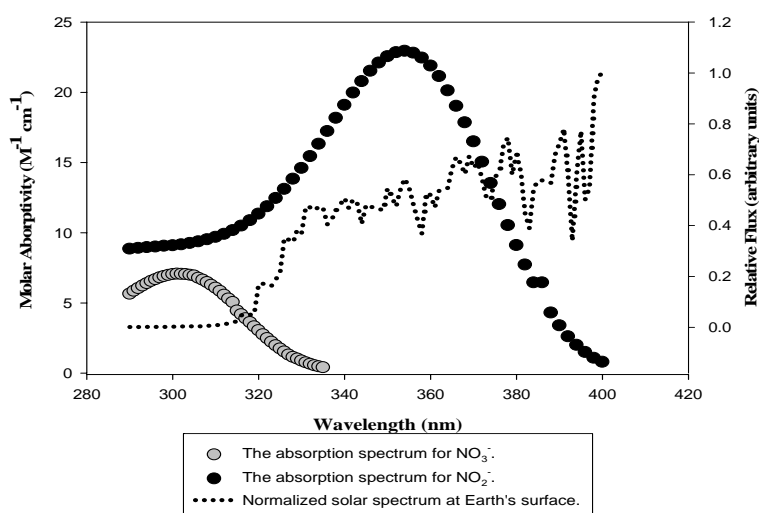
[d] $J_{NO_2^-}$ was extrapolated from Zuo and Deng, 1999.

[e] *volumetric* $\sim 4.65\times10^{-8}$ ($\frac{cm^3\,(QLL)}{cm^3\,(atmosphere)}$).

6030

Fig. 1. Simplified schematic diagram illustrating the primary reactions governing NO_x release from a 500 μm thick QLL film to the gas phase from nitrate photochemistry. At QLL depths ≤150 μm, NO_2 photolysis does not occur, while at QLL depths ≤150 μm NO_2 photolysis occurs.
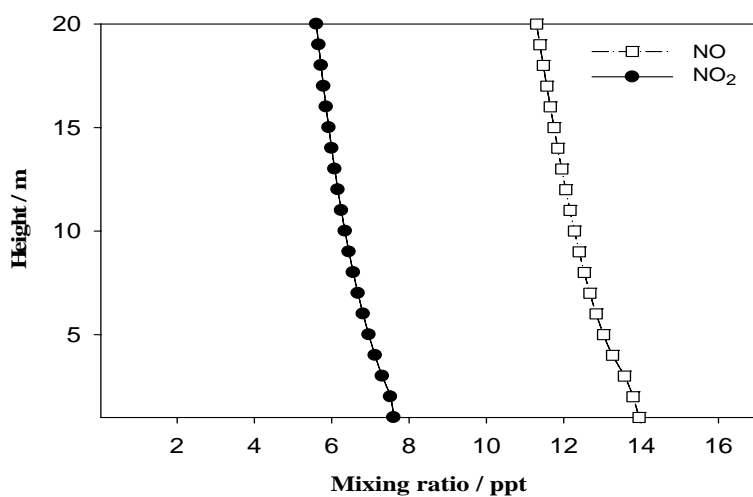
Fig. 2. The absorption spectrum for NO_3^- and NO_2^- (Gaffney et al., 1992; Zuo and Deng, 1998) and the normalized solar spectrum at the Earth's surface from 290 to 400 nm.
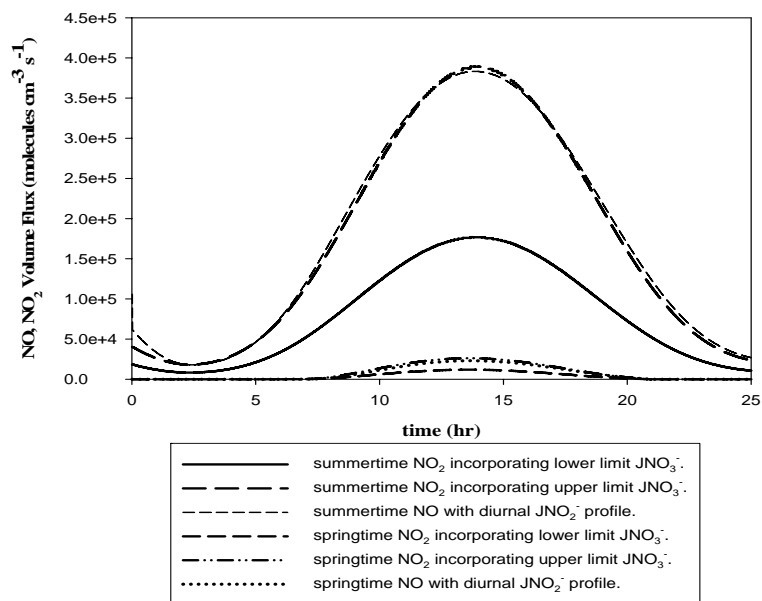
Fig. 3. Simulated diurnal summer and springtime volume flux profiles of NO and NO$_2$ just above the snowpack.

6033

Fig. 4. Calculated summertime gas phase NO and NO$_2$ concentration profiles as a function of height.